

Novel 3-Nitrotriazole-Based Amides and Carbinols as Bifunctional Antichagasic Agents

Maria V. Papadopoulou,^{*,†} William D. Bloomer,[†] Galina I. Lepesheva,[‡] Howard S. Rosenzweig,[§] Marcel Kaiser,^{||,⊥} Benjamín Aguilera-Venegas,^{#,∇} Shane R. Wilkinson,[∇] Eric Chatelain,[○] and Jean-Robert Ioset[○]

[†]NorthShore University HealthSystem, Evanston, Illinois 60201, United States

[‡]Department of Biochemistry, Vanderbilt University School of Medicine, Nashville, Tennessee 37232, United States

[§]Oakton Community College, Des Plaines, Illinois 60016, United States

^{||}Parasite Chemotherapy, Swiss Tropical and Public Health Institute, Basel, Switzerland

[⊥]University of Basel, Basel, Switzerland

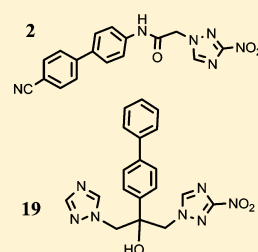
[#]Laboratory of Antioxidants, Institute of Nutrition and Food Technology, University of Chile, Santiago, Chile

[∇]School of Biological & Chemical Sciences, Queen Mary University of London, London, U.K.

[○]Drugs for Neglected Diseases initiative (DNDi), Geneva, Switzerland

Supporting Information

ABSTRACT: 3-Nitro-1H-1,2,4-triazole-based amides with a linear, rigid core and 3-nitrotriazole-based fluconazole analogues were synthesized as dual functioning antitrypanosomal agents. Such compounds are excellent substrates for type I nitroreductase (NTR) located in the mitochondrion of trypanosomatids and, at the same time, act as inhibitors of the sterol 14 α -demethylase (*T. cruzi* CYP51) enzyme. Because combination treatments against parasites are often superior to monotherapy, we believe that this emerging class of bifunctional compounds may introduce a new generation of antitrypanosomal drugs. In the present work, the synthesis and



Entry	IC ₅₀ (nM) <i>T. cruzi</i>	SI	TcNTR activity (nmol NAD/min/mg)
2	138	1194	888 +/- 24

19	33	3808	1160 +/- 19
-----------	----	------	-------------

Entry	<i>T. cruzi</i> CYP51 binding		
	K _d (μ M)	I/E ₂ (5 min)	I/E ₂ (1 h)
Fluconazole	0.230	<1	16
19	0.023	<1	3

in *vitro* and in *vivo* evaluation of such compounds is discussed.

INTRODUCTION

About one-sixth of the world's population, most living in developing countries, suffer from a series of infections collectively known as neglected tropical diseases (NTDs).¹ In addition to killing more than 500,000 people each year, these illnesses impair physical and cognitive development of children, make it difficult to farm or earn a living, and limit productivity in the workplace. Two NTDs are American trypanosomiasis (also known as Chagas disease), which is caused by the protozoan parasite *Trypanosoma cruzi* and is endemic in 21 countries across Latin America, and human African trypanosomiasis (HAT) (also known as African sleeping sickness), which is prevalent across sub-Saharan Africa and caused by *T. brucei rhodesiense* and *T. brucei gambiense*. Although the number of incidences of both infections has significantly declined in the past 20 years due to implementation of vector control initiatives, the diseases still remain a major global health issue, especially since the number of cases in nonendemic sites (United States, Australia, Europe, and Japan) is rising, primarily due to international population migration and transfusion of contaminated blood.^{2–4}

The therapeutic options for Chagas are currently limited to two drugs, both nitroheterocyclic compounds, nifurtimox (Nfx;

Lampit) and benznidazole (Bnz; Rochagan), while the success of treatment depends on the phase of the disease. Thus, cure rates of 65–80% can be achieved in the acute phase, whereas only 15–30% cure rates have been reported among adults in the chronic stage.^{5,6} Besides the low efficacy in patients with chronic disease, safety and tolerability issues are also major drawbacks for these drugs. Therefore, the development of new, safer, and more effective therapeutic treatments remains a key challenge for Chagas disease control.

Currently, inhibitors of the fungal sterol 14 α -demethylase enzyme (CYP51) represent a new form of treatment against Chagas disease and demonstrated promising efficacy in preclinical studies.^{7,8} Additional pathogen-specific drug discovery efforts have resulted in inhibitors for the orthologous enzyme *T. cruzi* CYP51 (TcCYP51).^{9–12} One such compound, VNI, showed parasitological cures in both the acute and chronic *in vivo* Chagas model.¹¹ However, the antifungal agent posaconazole revealed ~80% treatment failure in clinical trials in human patients with chronic Chagas disease, while Bnz was proven more efficacious.¹³ In addition, in newly designed *in*

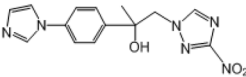
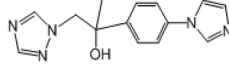
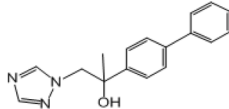
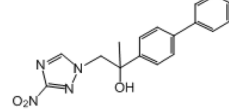
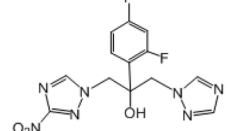
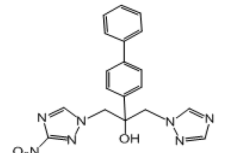
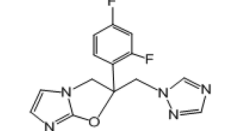
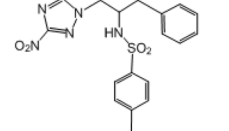
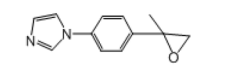
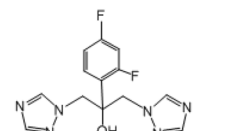
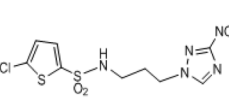
Received: October 13, 2014

Published: January 12, 2015

Table 1. *In Vitro* Antiparasitic Activity, Host Toxicity, and Physical Properties of Tested Compounds

ID No	<i>T. b. rhod.</i> ^a IC-50 μ M	SI	<i>T. cruzi</i> ^b IC-50 μ M	SI	Cytotox. L6 ^c IC-50 μ M	Chemical Structure	Bnz/comp	clogP	PSA (\AA^2)
Melars. 0.007 \pm 0.001									
Bnz 2.18 \pm 0.08									
2	0.336	490	0.138	1194	164.7		10.77	2.75	129.42
3	4.060	24	0.102	973	98.8		7.24	3.23	118.52
4	73.870		16.58	>16.5	> 273.6		0.04	2.33	131.41
5	0.901	140	0.045	2797	125.9		45.1	2.716	108.87
6	16.066		0.459	192	88.1		4.42	1.625	121.23
7	10		3.986	15.6	62.1		0.51	2.436	108.87
8	7.035	10	0.552	122	67.3		3.67	1.183	121.23
9	17.015		0.554	186	103.0		3.66	0.901	112.11
10	34.067		1.194	205.6	245.5		1.29	1.85	93.6
11	1.75	125	0.188	1164	219.5		11.9	3.21	93.6
12	51.71		22.775	4.9	112.6		2.393		45.03
13	76.55		14.229		9.7		3.048		84.48

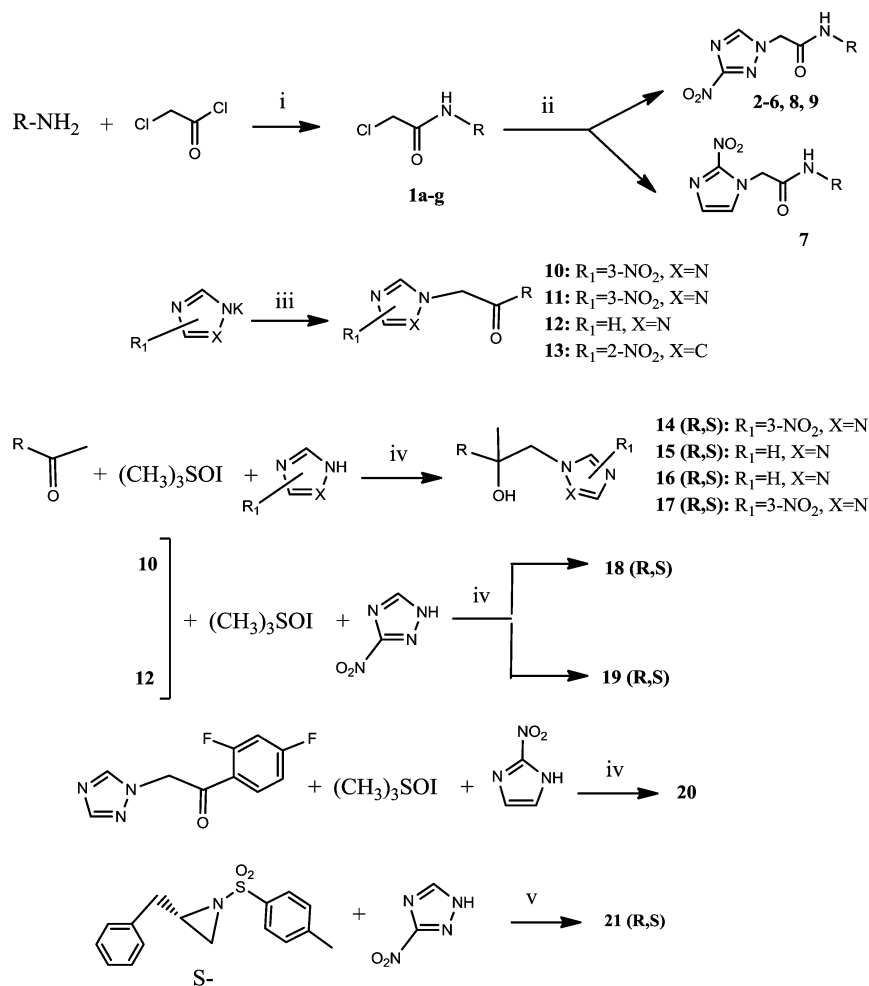
Table 1. continued

ID No	<i>T.b.rhod.</i> ^a IC-50 μ M	SI	<i>T. cruzi</i> ^b IC-50 μ M	SI	Cytotox. L6 ^c IC-50 μ M	Chemical Structure	Bnz/comp	clogP	PSA (\AA^2)
14	1.838	>173	3.29	>97	>318.5		0.68	0.54	114.58
15	153.16	>2.43	157.2	>2.4	>371.7			-0.09	68.76
16	65.6	1.74	0.706	161.9	114.3		3.17	2.74	50.94
17	1.09	78.9	0.102	844	86.0		21.94	3.36	96.76
18	26.610		1.174	220	258.4		1.81	1.18	127.47
19	2.877	44	0.033	3807.7	126.6		67.82	2.54	127.47
20	220.86		5.786	>49.4	>286.0		0.35	1.25	52.79
21	11.596		0.339	428	145.1		1.7	3.55	122.7
22	76.25	3.64	187.5	1.48	277.3			0.77	30.35
Fluconazole			9.967	>29.51	>294.1			0.56	81.65
23	1.99	122	0.438	556	243.5		3.6	1.74	122.7

^a*T.b. rhodesiense*, strain STIB 900 trypomastigotes. ^b*T. cruzi*, strain Tulahuen C4 amastigotes; SI is the ratio IC_{50} in L6 cells/ IC_{50} in each parasite. ^cCytotoxicity in host L6 cells. Reference drugs: Melarsoprol (Melars) and Benznidazole (Bnz). The IC_{50} value of each reference drug is the mean from multiple measurements in parallel with the compounds of interest. Active and moderately active compounds with acceptable selectivity are colored green and pink, respectively; compounds with an unacceptable selectivity are colored blue, whereas inactive compounds are colorless. PSA: polar surface area. All physical properties were predicted by using the Marvin Calculator (www.chemaxon.com). Values are means of 2 to 3 measurements. The SD was <5%. Data for compound 23 are taken from ref 17.

in vitro assays, nitroheterocyclic compounds were more efficacious trypanocidal agents than four different CYP51 inhibitors,

including antifungal drugs posaconazole and ravuconazole and two pyridine-based compounds,¹⁴ suggesting that inhibitors of

Scheme 1. Preparation of Compounds 2–21^a

^aReagents and conditions: i) Et₃N, CH₂Cl₂, RT; (ii) 3-nitro-1,2,4-triazole/2-nitroimidazole, KOH, CH₃CN, reflux 9 h; (iii) 3-nitro-1,2,4-triazole/2-nitroimidazole, KOH, CH₃CN, α -bromoketone, reflux 5–6 h; (iv) KOH in H₂O/2-propanol, reflux 1 h; (v) NaH (60%), propanol-1, reflux 6 h.

sterol biosynthesis may not be as efficient as single chemotherapeutic agents against Chagas disease as they are against fungal infections. Interestingly, a recent study with Bnz and posaconazole administered concomitantly or in sequence suggested a positive interaction between the two drugs, at least in an acute murine infection model.¹⁵

We have recently demonstrated that another class of nitroheterocyclic compounds, 3-nitro-1*H*-1,2,4-triazoles, are very potent antichagasic agents both *in vitro* and *in vivo*, whereas several analogues showed very good *in vitro* efficacy against *T. brucei rhodesiense* as well.^{16–19} These studies clearly demonstrated that 3-nitrotriazole-based compounds are significantly more potent and less toxic than their 2-nitroimidazole-based counterparts,^{19,20} with part of the trypanocidal activity being dependent on the parasite's expression of an oxygen-insensitive type I nitroreductase (NTR), an enzyme absent from most other eukaryotes.^{16,17,19} This same enzyme, via a series of two electron reduction reactions, which lead to the production of toxic metabolites, is responsible for the trypanocidal activity of Nfx, Bnz, and other nitroheterocyclic prodrugs in general.^{21–24}

In this work we examined the possibility of synthesizing dual-functioning 3-nitrotriazole-based compounds; such compounds could potentially act as prodrugs via their reducible nitro-group

and, at the same time, be inhibitors of CYP51 enzyme via their triazole-based scaffold.²⁵ The synthesis of bifunctional agents has the advantage of combining the beneficial effects of nitroheterocyclics with the beneficial effects of ergosterol biosynthesis inhibitors in one molecule. To accomplish this task, we synthesized and evaluated *in vitro* and *in vivo* linear, rigid 3-nitrotriazole-based amides and 3-nitrotriazole-based carbinols (analogues of fluconazole), as potential antitrypanosomal/antichagasic agents, NTR substrates, and TcCYP51 inhibitors.

On the basis of our previous work,^{16–19} we have realized that most 3-nitrotriazole-based analogues are very good substrates of NTR enzyme. Therefore, our goal was to obtain 3-nitrotriazole-based structures demonstrating affinity for CYP51. Early studies with 3-nitrotriazole-based amides having a flexible core showed lack of affinity for TcCYP51. Therefore, we assumed a more rigid, linear core should potentially provide a better fit in the active site of this enzyme. Thus, amides 2–8 were synthesized (Table 1). We chose the class of amides because they demonstrated better ADME properties than other 3-nitrotriazole-based compounds.¹⁹ Alternatively, the core of the CYP51 inhibitor fluconazole was used as a good starting point, and compounds 18–21 were synthesized (Table 1). Carbinols 14–17 were synthesized as structures that combine

the linearity and rigidity of the amides 2–8 and share some of the features of the fluconazole core.

RESULTS AND DISCUSSION

Chemistry. The structures of synthesized compounds are shown in Table 1. Their synthesis is straightforward and based on well-established chemistry outlined in Scheme 1. Thus, amides 2–9 were obtained by nucleophilic substitution of chloroacetamides 1a–g with the potassium salt of 3-nitrotriazole or 2-nitroimidazole under refluxing conditions. Similarly, nitro(triazole/imidazole)-ketones 10–13 were synthesized by nucleophilic substitution of α -bromoketones. Carbinols 14–19 were obtained in one step by using a modified Corey-Chaykovsky reaction;²⁶ in this one-pot reaction, trimethylsulfoxonium iodide was used in a 2-propanol/aqueous KOH (1:1) solution and the appropriate ketone was added to form *in situ* an oxirane; then 3-nitrotriazole was added followed by 1 h refluxing. Although the yields by using this method were low, the method is attractive due to its simplicity and short reaction time. The obtained carbinols 14–19 were used as racemic mixtures. When 2-nitroimidazole was used in the modified Corey-Chaykovsky reaction, the bicyclic compound 20 was formed as the final product, presumably via an intramolecular aromatic nucleophilic substitution of the nitro-group by the hydroxyl-group. The sulfonamide 21 was formed by nucleophilic attack of the sodium salt of 3-nitrotriazole with the appropriate aziridine-sulfonamide (Scheme 1).

Biological Evaluation. Antiparasitic Activity. Compounds were tested for antitrypanosomal activity against *T. cruzi* amastigotes and bloodstream form (BSF) of *T. b. rhodesiense*. Dose response curves were constructed from which the concentration of compound that inhibits parasite growth by 50% (IC_{50}) was calculated for each parasite (Table 1). In addition, compounds were tested for toxicity in L6 rat skeletal myoblasts, the host cells for *T. cruzi* amastigotes, in order to calculate a selectivity index for each parasite ($SI = IC_{50L6}/IC_{50parasite}$) (Table 1). The TDR (Special Programme for Research and Training in Tropical Diseases, World Health Organization) criteria for activity were adapted to interpret the data.²⁷ Thus, for *T. cruzi* amastigotes, an IC_{50} of $<4.0 \mu M$, between 4.0 and 60 μM , or $>60 \mu M$, designates “active,” “moderately active,” or “inactive” compounds, respectively, whereas for BSF *T. b. rhodesiense*, IC_{50} values of $<0.5 \mu M$, between 0.5 and 6.0 μM , or $>6.0 \mu M$ identify “active,” “moderately active,” or “inactive” compounds, respectively. In addition, SI values should ideally be ≥ 50 and ≥ 100 for *T. cruzi* and *T. b. rhodesiense*, respectively.²⁷

All the 3-nitrotriazole-based rigid amides (2, 3, 5, 6, 8, and 9) except 4, and all the 3-nitrotriazole-based carbinols (14 and 17–19), as well as the fluconazole-like 3-nitrotriazole-based sulfonamide 21, were active antichagasic agents with acceptable selectivity indices (Table 1). Only three compounds (two 3-nitrotriazole-based amides and one 3-nitrotriazole-based carbinol) were active (2) or moderately active (5 and 14) anti-HAT agents with acceptable SI values. In addition, ketone 11, the precursor of carbinol 19 showed a moderate anti-HAT activity with acceptable selectivity. As observed before, compound 7, the 2-nitroimidazole-based analogue of 6, was borderline active against *T. cruzi* amastigotes but with an unacceptable SI value (Table 1).

Analysis of Antichagasic Activity. Linear, Rigid Amides 2–9. Although a detailed SAR evaluation cannot be conducted

due to the limited number of compounds studied, we made the following observations: A chloro-substituent in the para position of a diphenyl-core in the rigid amide 5 increased the efficacy against *T. cruzi* by a factor of 3 compared to the cyano-substituted analogue 2. Although 5 was slightly more toxic to L6 cells than compound 2, its SI for *T. cruzi* was also increased about 2-fold compared to 2 due to its better antichagasic efficacy; this cannot be attributed to lipophilicity since both compounds share similar clogP values, but perhaps to its lower PSA value (Table 1). Chloro-substitution in the phenylthiazole-core of 3 was also beneficial for its antichagasic activity and selectivity compared to the difluoro-substitution in the analogue 6. However, in this case, increased antichagasic efficacy may be related to the increased lipophilicity of 3 compared to 6. Reversing the order between the thiazole and phenyl rings in amide 8 slightly decreased antichagasic activity compared to 6, and once again, this reduction may be related to slightly lower lipophilicity compared to 6. Furthermore, this reversal lead to a slightly more toxic compound (compare 8 to 3 and 6). Replacing the terminal phenyl ring in the biphenyl core of 2 or 5 with a piperidinic group in 9 resulted in reduced efficacy against *T. cruzi*, which seems to be attributed to a decreased clogP value (Table 1). Compound 4 with a thiodiazole ring in the rigid core failed to show either good antichagasic activity or acceptable selectivity. However, compound 4 has significant solubility problems and may have not been evaluated properly. Although compound 7, the 2-nitroimidazole analogue of 6, showed borderline antichagasic activity according to the TDR criteria, it was the most toxic rigid amide in L6 cells and failed to show an acceptable SI for *T. cruzi*. Compound 7 was about 8.7-fold less active against *T. cruzi* compared to its 3-nitrotriazole analogue 6, even though the latter was 1.5 times less lipophilic, suggesting that the reason for the reduced antichagasic activity of 7 was related to the 2-nitroimidazole ring. All 3-nitrotriazole-based rigid amides, except 4, were more potent antichagasic agents than Bnz, with compound 5 being 45-fold more potent than Bnz (Table 1).

Carbinols and Their Precursors. With regard to the carbinols in Table 1, which were racemic mixtures, we observe the following: Lipophilicity and the presence of the nitro-group in the triazole-ring played a significant role in the antichagasic activity. Thus, the 3-nitrotriazole-based carbinol 14, with a terminal imidazole ring in the core, was significantly less lipophilic than carbinol 17, with a terminal phenyl ring in the core, and 32-fold less potent against *T. cruzi* amastigotes than 17 (Table 1). Carbinol 15, the analogue of 14 without the 3-nitro-group in the triazole ring, had a negative clogP value and was inactive against *T. cruzi*. Interestingly, carbinol 16, the analogue of 17 without the 3-nitro group in the triazole ring, was still active against *T. cruzi*, most likely because of its relatively high lipophilicity. However, the lack of the nitro-group resulted in a 7-fold reduction in antichagasic potency compared to 17. Carbinol 18 is the mononitrotriazole analogue of fluconazole. This compound was 36-fold less potent than its more lipophilic analogue 19, which has an additional phenyl ring in the side chain. However, compound 18 was 8.5-fold more potent than fluconazole, which is less lipophilic and lacks the nitro-group (Table 1). Carbinol 19 was the most potent antichagasic compound tested and demonstrated the highest SI value. In addition, 19 was about 68-fold more potent than Bnz (Table 1). The bicyclic compound 20 was formed *in situ* from the corresponding 2-nitroimidazole analogue of fluconazole presumably by intramolecular nucleophilic aromatic substitu-

tion of the nitro-group by the hydroxyl group. This compound, although slightly more lipophilic than **18**, was about 5-fold less potent against *T. cruzi*, presumably because it lacks the nitro group. In addition, compound **20** was moderately active and marginally selective (SI > 49.4) for *T. cruzi* parasite. In compound **21** we replaced the hydroxyl-group with a tosylamino-group. Compound **21** was selectively active against *T. cruzi*, but its potency was about 3-fold less compared to carbinol **17** with a similar lipophilicity. An increased PSA value compared to **17** may have played a role for this reduction in this case.

Some ketones, precursors of the carbinols in Table 1, were also evaluated for antichagasic activity. Interestingly, the 3-nitrotriazole-based ketones **10** and **11**, precursors of carbinols **18** and **19**, respectively, were found to be selectively active against *T. cruzi* (Table 1). The pattern of lipophilicity and the presence of the nitro-group in the triazole ring were consistent with our predictions for efficacy. Thus, the more lipophilic **11** was more potent than **10**, whereas ketone **12**, the analogue of **11** without the nitro-group, was only moderately active against *T. cruzi* and did not fulfill the TDR selectivity criteria. Once again, the 2-nitroimidazole analogue of **11**, ketone **13**, was only moderately active against *T. cruzi* parasites, but also the most toxic compound to the host cells. From this evaluation, it appears that 3-nitrotriazole-based ketones represent another class of antichagasic agents. Finally, compound **22**, the precursor of carbinols **14** and **15**, was inactive against *T. cruzi* (Table 1).

Analysis of Anti-HAT Activity. Linear, Rigid Amides 2–9. With regard to the anti-HAT activity of amides 2–9, biphenyl amides **2** and **5** (which were active and moderately active, respectively) were more potent against *T. b. rhodesiense* than phenylthiazole-amides **3**, **6**, **7**, and **8**. In fact, none of the latter demonstrated an acceptable selective anti-HAT activity (Table 1). The phenyl-thiodiazoleamide **4** did not show any anti-HAT activity, in part due to solubility issues as mentioned earlier, whereas the piperidinophenylamide **9** was inactive, perhaps because of planarity issues in the side chain. Interestingly, the 2-nitroimidazole-based phenylthiazole-amide **7** demonstrated a lower IC₅₀ value against *T. b. rhodesiense* than its 3-nitrotriazole-based analogue **6**, possibly due to the higher lipophilicity of the first. Nonetheless, both were inactive against this parasite.

Carbinols and Their Precursors. Only carbinol **14** was moderately active with acceptable selectivity against *T. b. rhodesiense*. Carbinol **17** with increased lipophilicity was more active than **14** but not selective enough for this parasite. Similarly, carbinol **19** was more active than the less lipophilic analogue **18**, but also lacked an acceptable selectivity for *T. b. rhodesiense*. Linear, rigid carbinols lacking the nitro-group (**15** and **16**) were inactive against *T. b. rhodesiense*. Interestingly, the precursor of carbinol **19**, the lipophilic enough 3-nitrotriazole-based ketone **11**, was moderately active and had an acceptable selectivity for *T. b. rhodesiense*.

Involvement of Type I Nitroreductase. Representative 3-nitrotriazole-based linear rigid amides and carbinols, with IC₅₀ values against *T. cruzi* ranging from 33 nM to 3.29 μM, were evaluated as substrates of recombinant TbNTR and TcNTR enzymes (Table 2). Enzyme specific activity was measured as oxidized NADH per min per mg of protein. All tested nitrotriazoles were excellent substrates of Tb and TcNTR enzymes. Thus, tested nitrotriazoles were metabolized by Tb and TcNTR at rates approximately 2-fold higher than Bnz, whereas TbNTR can metabolize nitrotriazoles (and Bnz) at

Table 2. Enzymatic Activity of Recombinant TbNTR and TcNTR toward Bnz and Representative 3-Nitrotriazoles from Table 1^a

compd	specific activity values (nmol NADH oxidized per min per mg NTR)	
	TbNTR	TcNTR
Bnz	1540 ± 67	680 ± 8
2	3172 ± 11	888 ± 24
14	3456 ± 6	1067 ± 16
18	3063 ± 43	1178 ± 10
19	2681 ± 21	1160 ± 19

^aA precipitation issue occurred with compound **2** in the assay buffer used. Enzyme assays were carried out in triplicate and repeated twice.

rates 2- to 3-fold greater than those of TcNTR. In addition, bloodstream form *T. b. brucei* parasites overexpressing TbNTR were 2- to 3-fold more susceptible to compound **2** compared to parasites not induced to express elevated levels of TbNTR (IC₅₀: 0.36 ± 0.01 vs 0.84 ± 0.16). However, no correlation existed between parasitic IC₅₀ values (Table 1) and activation rate by TcNTR or TbNTR, suggesting that antiparasitic activity was not exclusively dependent on NTR-induced activation.

TcCYP51 Inhibition. Azole-based scaffolds are effective inhibitors of the *T. cruzi* enzyme sterol 14α-demethylase (TcCYP51).²⁵ By using eburicol as substrate, TcCYP51 is a central enzyme in parasitic sterol biosynthesis, an essential pathway in all life stages of *T. cruzi* for the formation of ergosterol and related structures from lanosterol.^{28,29} Being azoles, our compounds could be potential inhibitors of TcCYP51. Moreover, reduction of the nitro-group by P450 reductase (which normally reduces the Fe³⁺ to Fe²⁺ in the heme cofactor of CYP51) could potentially cause irreversible binding to the protein. Benzimidazole was found to be an irreversible inhibitor of TcCYP51, although with weak affinity for the enzyme.³⁰ Binding of a heterocyclic compound to CYP51 can be quantified spectroscopically by measuring a dose-response type 2 shift that occurs upon coordination of a Lewis-base atom of the ligand to the heme iron of the enzyme.⁹ The first 3-nitrotriazole-based compound we tested as a potential TcCYP51 ligand was chlorothiophene-2-sulfonamide **23**, with a flexible core (Table 1). The biological properties of **23** have been described before¹⁷ and are included in Table 1 for reference. This compound displayed a weak affinity toward TcCYP51, providing a high K_d value of 65.2 ± 5.3 (Table 3). Therefore, we assumed that compounds with a more rigid core could better fit in the active site of the enzyme and thus act as stronger inhibitors. Indeed, compound **2** with a linear rigid core

Table 3. Binding of Compounds to Recombinant *T. cruzi* CYP51^a

compd	K _d (μM)	I/E ₂ (5 min)	I/E ₂ (1 h)
2	ND	4	36
18	0.606 ± 0.023	5	32
19	0.023 ± 0.012	<1	3
23	65.2 ± 5.3	ND	ND
fluconazole	0.230 ± 0.029	<1	16
Bnz ^b	ND	43.2	45

^aK_d: Dissociation constant. I/E₂: Molar ratio of inhibitor/enzyme, which causes a 2-fold decrease in enzyme activity in 5 min and 1 h reactions. ND: not determined. ^bValues for Bnz were taken from ref 30.

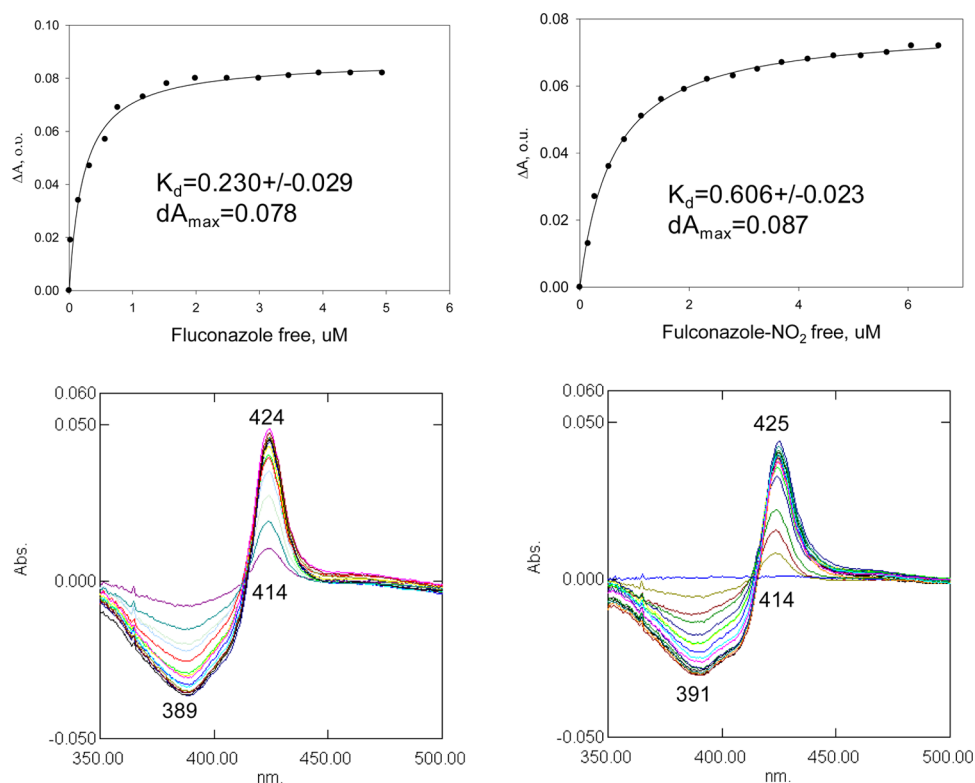


Figure 1. Binding of fluconazole and compound **18** (NO₂-fluconazole) to *T. cruzi* CYP51. Both compounds produce typical type 2 spectral response in *T. cruzi* CYP51, indicating at least initial coordination of triazole N4 to the P450 heme iron. However, compound **18** is a weaker binder.

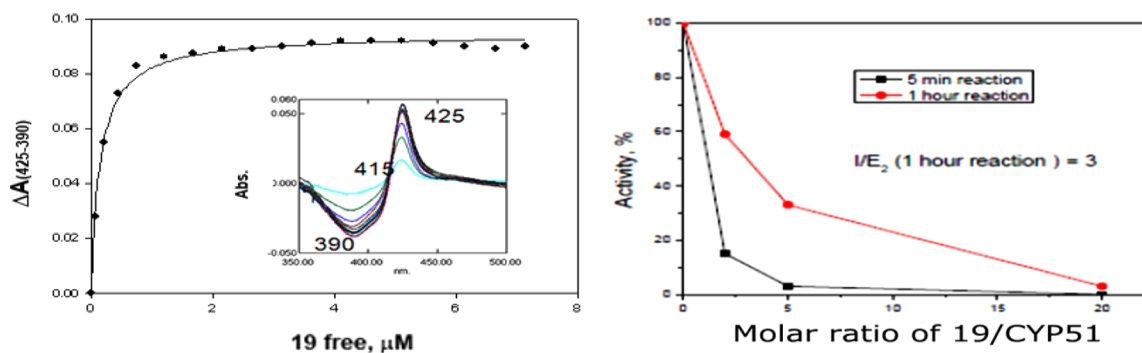


Figure 2. Binding (left panel) and inhibition (right panel) of *T. cruzi* CYP51 by compound **19** in 5 min and 1 h reactions. The same results were obtained independently of the sequence that substrate eburicol (S) or inhibitor (I) were added, namely: reaction mixture + I/+NADPH, 5 min incubation at 37 °C /+S or, Reaction mixture + I + S /+NADPH.

inhibited the enzyme with an initial I/E_2 ratio (molar ratio of inhibitor/enzyme, which causes a 2-fold decrease in enzyme activity) of 4 in a 5 min reaction. However, this ratio was increased to 36 in the 1 h reaction, indicating that inhibition by **2** was reversible. The 3-nitro-triazole-fluconazole analogue **18** binds to TcCYP51 and induces the same typical type 2 spectral response as fluconazole (Figure 1), indicating at least initial coordination of the triazole N4 to the P450 heme iron.⁹ However, **18** was a weaker binder than fluconazole (K_d 0.606 versus 0.230 μM) (Table 3). To the contrary, carbinol **19**, an analogue of fluconazole with an elongated rigid side chain, elicited the spectral response in TcCYP51 with an apparent K_d 10-fold stronger than fluconazole. In the reconstituted CYP51 reaction, **19** produced I/E_2 ratios of <1 and 3, in 5 min and 1 h reactions, respectively (Table 3 and Figure 2). Furthermore, for carbinol **19** at high I/E ratios (≥ 20), the inhibition seems to be irreversible, although further experiments are needed for

verification (Figure 2). Correlation exists between *in vitro* antichagasic potency and inhibition of TcCYP51 for the nitro-compounds **2**, **19**, and **23**. However, compound **18** was more potent in killing *T. cruzi* amastigotes than fluconazole (Tables 1), although the latter was a stronger TcCYP51 inhibitor (Table 3). This might be related to the nitro-group of **18**, making this compound bifunctional. Crystallography studies could shed more light on the orientation of these bifunctional agents in the TcCYP51 active site.

In Vivo Antichagasic Activity. Compounds **2**, **5**, **18**, and **19** were evaluated for *in vivo* antichagasic activity by using an acute *T. cruzi* infected murine model as described before.¹⁹ Bnz was used in parallel as a positive control. Infected mice (5 mice/group) were treated i.p. for up to 10 consecutive days with each compound, at 15 mg/kg/day, except for compound **5**, which was administered at 13 mg/kg/day. The parasite index (PI), which is an indicator for parasite clearance, was calculated after

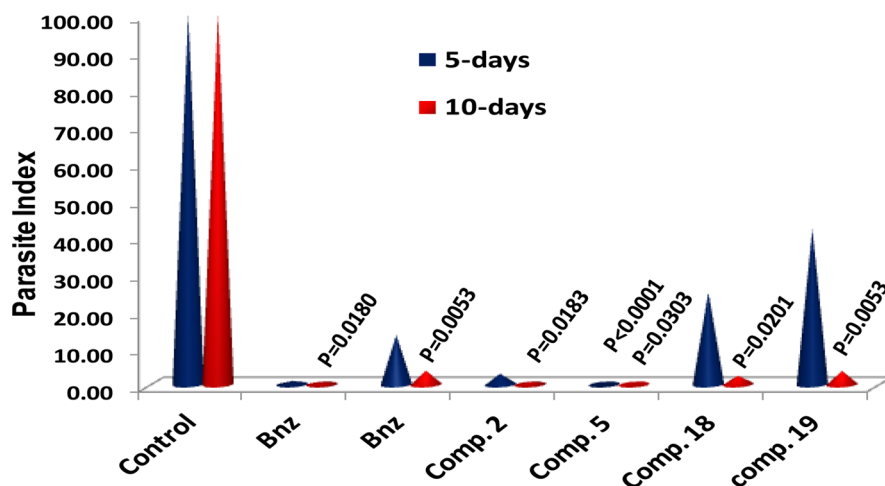


Figure 3. *In vivo* evaluation of the antichagasic efficacy of compounds 2, 5, 18, and 19 in the acute murine model. Benznidazole (Bnz) data from two experiments in parallel were included. All compounds except 5 were administered (i.p.) at 15 mg/kg/day. Compound 5 was administered (i.p.) at 13 mg/kg/day. The *P* values refer to comparisons between treated groups and control group. When *P* values are not given, there was no statistical difference. Groups of 5 mice/group were used. Occasionally, 10 mice were used in the control group.

5 and 10 days of treatment.¹⁹ The data from these studies are summarized in Figure 3. All tested compounds reduced the PI to <4% after 10-day treatment with statistical significance compared to the 10-day untreated control. The linear rigid amides 2 and 5 were able to reduce parasites to undetectable levels even after 5 days of treatment. However, only compound 5 yielded a statistically significant different PI value compared to untreated control after 5 days of treatment ($P < 0.0001$), whereas for Bnz and compound 2 (treated in the same experiment) the corresponding *P* value was 0.080 and 0.0819, respectively. Carbinols 18 and 19 provided a PI value of 24.9 and 42.04, respectively, after 5-day administration but without statistical significance compared to the untreated control ($P = 0.1680$ and 0.2706 , respectively). Bnz in this latter experiment provided a PI value of 13.38 after 5-day treatment, also not statistically different from the untreated control ($P = 0.2706$). None of the tested compounds were toxic to mice at the given doses and administration schedule.

***In Vitro* ADME Studies.** To understand better the *in vivo* activity of compounds 2 and 19 and explain the discrepancy between *in vitro* and *in vivo* potency, we performed some *in vitro* ADME studies (Table 4). Compound 2 represents the linear rigid amides and 19 the carbinols. Both compounds demonstrate high Caco-2 perm ability³¹ and similar metabolic stability in the presence of murine or human microsomes. Both compounds were quite stable, explaining their good *in vivo* activity after 10-day dosing. The fact that compound 19 was acting slower than 2 may be related to its stronger binding to TcCYP51, a membrane protein, whereas type I NTR is mitochondrial based. Thus, if compound metabolites formed through NTR-activation are the most toxic chemical species for *T. cruzi*, compound 2 would be expected to act faster than 19. Obviously, additional pharmacokinetic parameters (such as volume distribution and protein binding), which can affect the *in vivo* behavior of these compounds, cannot be excluded.

It is concluded from the above data that 3-nitrotriazole-based linear rigid amides and carbinols are potent antichagasic agents via their dual functioning properties as substrates for trypanosomal type I NTR and as inhibitors of CYP51. In addition, these compounds demonstrate excellent Caco-2 permeability and metabolic stability in the presence of human

Table 4. *In Vitro* ADME Data for Compounds 2 and 19^a

compd	mean A → B P_{app} ($\times 10^{-6}$ cm s ⁻¹)	test species	mean remaining parent, with NADPH (%)	mean remaining parent, free of NADPH (%)
2	18.7	human	96.8	84.8
		mouse	79.4	110
19	16.5	human	90.7	106
		mouse	77.6	102
verapamil		human	8.4	89.4
		mouse	6.0	96.5
warfarin	25.3	human	102	96.7
		mouse	104	101
ranitidine	0.24			

^a P_{app} : Caco-2 apparent permeability. Permeability ranking: low, <0.5; moderate, 0.5–5; high, >5. For permeability measurements, 10 μ M concentration and 2 h assay time were used. For metabolic stability, 1 μ M concentration and 0 and 60 min incubation time were used. Test species represent either human or mouse microsomes.

or murine microsomes. Carbinols were slower in clearing the parasites *in vivo* compared to the linear rigid amides; however, both types of compounds were able to clear *T. cruzi* after 10-day treatment. This is apparent in the images shown in Figure 4. We have also shown previously that 3-nitrotriazole-based compounds are not mutagenic compared to their 2-nitroimidazole-based analogues¹⁹ and do not cause developmental toxicity in zebrafish.²⁰

In comparison with some monofunctional 3-nitrotriazole-based analogues, there is no substantial difference in antichagasic *in vitro* activity. Thus, we have seen *in vitro* IC₅₀ values against *T. cruzi* amastigotes at low nanomolar concentrations with several 3-nitrotriazole-based amides/sulfonamides or piperazines, which, having a more flexible core, did not demonstrate affinity for TcCYP51.^{17–19} In the present work, the bifunctional compounds that have been tested *in vivo* were able to completely clear the parasites after 10-day treatment, something that was not always achievable with monofunctional 3-nitrotriazole-based derivatives.¹⁹ However, since *in vitro* activity does not always translate to *in vivo* efficacy, due to pharmacokinetic/pharmacodynamic factors,¹⁹

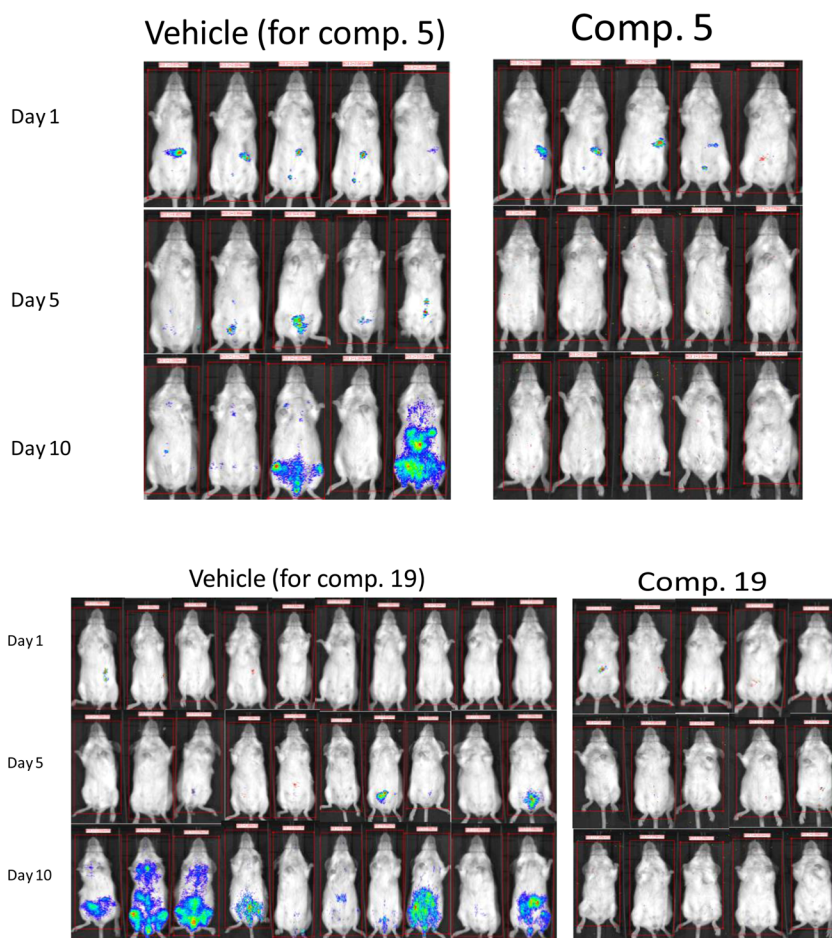


Figure 4. Images from mice treated with vehicle or compounds 5 and 19.

and since activity in the acute model does not guarantee cures, future experiments in a chronic murine model are necessary to determine the validity of these bifunctional compounds for the treatment of Chagas disease.

EXPERIMENTAL SECTION

Chemistry. General. All starting materials and solvents were purchased from Sigma-Aldrich (Milwaukee, WI), were of research-grade quality, and were used without further purification. Solvents used were anhydrous, and the reactions were carried out under a nitrogen atmosphere and exclusion of moisture. Melting points were determined by using a Mel-Temp II Laboratory Devices apparatus (Holliston, MA) and are uncorrected. Proton NMR spectra were obtained on a Varian Inova-500 or an Agilent Hg-400 spectrometer at 500 or 400 MHz, respectively, and were referenced to Me₄Si or to the corresponding solvent if the solvent was not CDCl₃. High-resolution electrospray ionization (HRESIMS) mass spectra were obtained on a Agilent 6210 LC-TOF mass spectrometer at 11000 resolution. Thin-layer chromatography was carried out on aluminum oxide N/UV₂₅₄ or polygram silica gel G/UV₂₅₄ coated plates (0.2 mm, Analtech, Newark, DE). Chromatography was carried out on preparative TLC alumina GF (1000 μm) or silica gel GF (1500 μm) plates (Analtech). All compounds were purified by preparative TLC chromatography on silica gel or alumina plates and also checked by HPLC (≥95% purity).

Synthesis of Chlorides 1a–g. Some of the chlorides 1a–g are known in the literature, and others are unknown or known through libraries but without any reference. The synthesis and spectroscopic data of 1a–g are provided in the Supporting Information.

General Synthetic Procedure of Amides 2–9. The potassium salt of 3-nitro-1,2,4-triazole or 2-nitroimidazole (1 equiv) was formed in CH₃CN (6–10 mL), by refluxing with KOH (1.2 equiv) for 30 min.

To this suspension 1a–g (1.1 equiv) was added, and the reaction mixture was refluxed under a nitrogen atmosphere for 9 h. In certain cases, 1a–g was added in CH₃CN solution. The reaction mixture was checked by TLC for completion of the reaction, and the solvent was evaporated. The residue was dissolved in ethyl acetate and the inorganic salts were filtered away. Upon preparative TLC (silica gel or alumina, depending on the mobility of the major band; ethyl acetate/petroleum ether), the desired product was obtained usually as a powder. Purity was checked also by HPLC and it was >95%.

N-[4-(4-Cyanophenyl)phenyl]-2-(3-nitro-1H-1,2,4-triazol-1-yl)acetamide (2). White microcrystalline powder (80%): mp 235 °C (dec); ¹H NMR (500 MHz, (CD₃)₂CO) δ 9.84 (br s, 1H), 8.76 (s, 1H), 7.90–7.75 (m, 8H), 5.46 (s, 2H). HRESIMS calcd for C₁₇H₁₃N₆O₃ and C₁₇H₁₂N₆NaO₃ *m/z* [M + H]⁺ and [M + Na]⁺ 349.1044 and 371.0863, found 349.1056 and 371.0873.

N-[4-(4-Chlorophenyl)-1,3-thiazol-2-yl]-2-(3-nitro-1H-1,2,4-triazol-1-yl)acetamide (3). White powder (64%): mp >235 °C; ¹H NMR (500 MHz, (CD₃)₂CO) δ 8.82 (s, 1H), 7.95 (d, *J* = 8.5 Hz, 2H), 7.64 (s, 1H), 7.46 (d, *J* = 8.5 Hz, 2H), 5.70 (s, 2H). HRESIMS calcd for C₁₃H₁₀ClN₆O₃S and C₁₃H₉ClN₆NaO₃S *m/z* [M + H]⁺ and [M + Na]⁺ 365.0218, 367.0191 and 387.0038, 389.0011, found 365.0231, 367.0200, and 387.0038, 389.0012.

N-[5-(4-Chlorophenyl)-1,3,4-thiadiazol-2-yl]-2-(3-nitro-1H-1,2,4-triazol-1-yl)acetamide (4). White powder (63%): mp >235 °C; ¹H NMR (500 MHz, DMSO-*d*₆) δ 8.93 (s, 1H), 7.96 (d, *J* = 8.5 Hz, 2H), 7.60 (d, *J* = 8.5 Hz, 2H), 5.57 (s, 2H). HRESIMS calcd for C₁₄H₁₁ClN₄O₄S *m/z* [M + H]⁺ 366.0184, 368.0148, found 366.0178, 368.0158.

N-(4'-Chloro-[1,1'-biphenyl]-4-yl)-2-(3-nitro-1H-1,2,4-triazol-1-yl)acetamide (5). Off-white powder (77%): mp >245 °C; ¹H NMR (500 MHz, CD₃OD + a drop of DMSO-*d*₆) δ 8.73 (s, 1H), 7.69 (d, *J* = 9.0 Hz, 2H), 7.61 (dd, *J* = 9.0, 4.0 Hz, 4H), 7.43 (d, *J* = 8.0 Hz, 2H),

5.32 (s, 2H). HRESIMS calcd for $C_{16}H_{11}ClN_3O_3$ m/z $[M - H]^-$ 356.05556, found 356.0563.

N-(4-(3,4-Difluorophenyl)thiazol-2-yl)-2-(3-nitro-1*H*-1,2,4-triazol-1-yl)acetamide (**6**). White powder (60%): mp 169–171 °C; 1H NMR (500 MHz, $(CD_3)_2CO$) δ 11.71 (br s, 1H), 8.80 (s, 1H), 7.83 (ddd, $J = 14, 7.5, 2$ Hz, 1H), 7.76 (m, 1H), 7.64 (s, 1H), 7.37 (dd, $J = 19, 8.5$ Hz, 1H), 5.69 (s, 2H). HRESIMS calcd for $C_{13}H_9F_2N_6O_3S$ m/z $[M + H]^+$ 367.0419, found 367.0426.

N-(4-(3,4-Difluorophenyl)thiazol-2-yl)-2-(2-nitro-1*H*-imidazol-1-yl)acetamide (**7**). Off-white powder (55%): mp 180–183 °C (dec); 1H NMR (500 MHz, $(CD_3)_2CO$) δ 11.70 (br s, 1H), 7.82 (ddd, $J = 12, 7.5, 2.5$ Hz, 1H), 7.77 (m, 1H), 7.63 (s, 1H), 7.61 (s, 1H), 7.36 (ddd, $J = 16.5, 10.5, 8.5$ Hz, 1H), 7.22 (s, 1H), 5.70 (s, 2H). HRESIMS calcd for $C_{14}H_{10}F_2N_5O_3S$ and $C_{14}H_9F_2N_5NaO_3S$ m/z $[M + H]^+$ and $[M + Na]^+$ 366.0467 and 388.0286, found 366.0466 and 388.0281.

N-(3-(2-Methylthiazol-4-yl)phenyl)-2-(3-nitro-1*H*-1,2,4-triazol-1-yl)acetamide (**8**). White, sticky solid (73%): mp 114–115 °C (dec); 1H NMR (400 MHz, $CDCl_3 + 2$ drops $DMSO-d_6$) δ 10.39 (s, 1H), 8.61 (s, 1H), 8.11 (s, 1H), 7.62 (d, $J = 7.6$ Hz, 2H), 7.39 (s, 1H), 7.36 (t, $J = 8.0$ Hz, 1H), 5.27 (s, 2H), 2.75 (s, 3H). HRESIMS calcd for $C_{14}H_{13}N_6O_3S$ m/z $[M + H]^+$ 345.0764, found 345.0776.

2-(3-Nitro-1*H*-1,2,4-triazol-1-yl)-*N*-(4-(piperidin-1-yl)phenyl)acetamide (**9**). Orange microcrystals (79%): mp 180–182 °C (dec); 1H NMR (400 MHz, $CDCl_3 + 1$ drop $DMSO-d_6$) δ 9.19 (br s, 1H), 8.44 (s, 1H), 7.37 (d, $J = 9.0$ Hz, 2H), 6.87 (d, $J = 9.0$ Hz, 2H), 5.10 (s, 2H), 3.10 (t, $J = 5.5$ Hz, 4H), 1.68 (m, 4H), 1.57 (m, 2H). HRESIMS calcd for $C_{15}H_{19}N_6O_3$ m/z $[M + H]^+$ 331.1513, found 331.1523.

General Synthetic Procedure of ketones 10–13. As in the case of amides 2–9, the potassium salt of 3-nitro-1,2,4-triazole or 2-nitroimidazole or 1,2,4-triazole (1 equiv) was formed in CH_3CN (6–10 mL), by refluxing with KOH (1.2 equiv) for 30 min, and the appropriate α -bromoketone (1 equiv) was added to this suspension. The reaction mixture was refluxed under nitrogen atmosphere for 5–6 h. The procedure for separation of the desired ketones 10–13 was analogous to that used for amides 2–9.

1-(2,4-Difluorophenyl)-2-(3-nitro-1*H*-1,2,4-triazol-1-yl)ethan-1-one (**10**). White crystals (85%): mp 102–104 °C; 1H NMR (500 MHz, $CDCl_3$) δ 8.30 (s, 1H), 8.09 (dd, $J = 9.0, 7.0$ Hz, 1H), 7.10 (td, $J = 9.5, 2.5$ Hz, 1H), 7.02 (td, $J = 9.0, 2.5$ Hz, 1H), 5.69 (d, $J = 3.0$ Hz, 2H). HRESIMS calcd for $C_{10}H_7F_2N_4O_3$ m/z $[M + H]^+$ 269.0481, found 269.0487.

1-(4-Phenylphenyl)-2-(1*H*-1,2,4-triazol-1-yl)ethan-1-one (**11**). White powder (95%): mp 175–177 °C; 1H NMR [500 MHz, $(CD_3)_2CO$] δ 8.67 (s, 1H), 8.16 (d, $J = 8.5, 2$ Hz), 7.84 (d, $J = 8.5, 2$ Hz), 7.70 (d, $J = 7.5, 2$ Hz), 7.48 (t, $J = 7.5, 2$ Hz), 7.41 (t, $J = 7.5, 1$ Hz), 6.15 (s, 2H). HRESIMS calcd for $C_{16}H_{13}N_4O_3$ and $C_{16}H_{12}N_4NaO_3$ m/z $[M + H]^+$ and $[M + Na]^+$ 309.0982 and 331.0802, found 309.0983 and 331.0804.

1-(4-Phenylphenyl)-2-(1*H*-1,2,4-triazol-1-yl)ethan-1-one (**12**). White microcrystals (65%; higher yield based on recovered ketone): mp 159–161 °C; 1H NMR (400 MHz, $CDCl_3$) δ 8.28 (s, 1H), 8.07 (d, $J = 8.8$ Hz, 2H), 8.03 (s, 1H), 7.76 (d, $J = 8.8$ Hz, 2H), 7.64 (d, $J = 6.8$ Hz, 2H), 7.52–7.44 (m, 3H), 5.71 (s, 2H). HRESIMS calcd for $C_{16}H_{14}N_3O$ m/z $[M + H]^+$ 264.1131, found 264.1154.

2-(2-Nitro-1*H*-imidazol-1-yl)-1-(4-phenylphenyl)ethan-1-one (**13**). White powder (60%): mp 163–164 °C; 1H NMR [500 MHz, $(CD_3)_2CO$] δ 8.20 (d, $J = 9.0$ Hz, 2H), 7.92 (d, $J = 9.0$ Hz, 2H), 7.78 (d, $J = 7.0$ Hz, 2H), 7.57 (d, $J = 1.0$ Hz, 1H), 7.53 (t, $J = 7.5$ Hz, 2H), 7.46 (t, $J = 7.5$ Hz, 1H), 7.23 (d, $J = 1.0$ Hz, 1H), 6.26 (s, 2H). HRESIMS calcd for $C_{17}H_{14}N_3O_3$ m/z $[M + H]^+$ 308.1030, found 308.1028.

General Synthetic Procedure of Carbinols 14–19 and Compound 20. The Corey–Chaykovsky reaction was applied for this synthesis, and a one-pot reaction was adapted from an international patent²⁶ because of its short time, albeit with low yields. Briefly, in a two-necked 25 mL round-bottom flask, KOH (2.4 equiv) was dissolved in 3 mL of distilled water, and an equal volume of 2-propanol was added. Trimethylsulfoxonium iodide (1.2 equiv) was added and stirred for 15 min under a nitrogen atmosphere. Then, the

appropriate ketone (1 equiv) was added, and stirring was continued for 15 min. Finally, 3-nitro-1,2,4-triazole, 2-nitroimidazole, or 1,2,4-triazole (1.2 equiv) was added, and the reaction mixture was refluxed for 1 h. 2-Propanol was evaporated, and the aqueous solution was neutralized with 1% HCl. This solution was then extracted with dichloromethane, and the organic layer washed with $NaHCO_3$ solution. The organic layer was dried over Na_2SO_4 and chromatographed by preparative TLC (silica gel, ethyl acetate plus 1% MeOH). When 2-nitroimidazole was used in the reaction mixture, a nucleophilic aromatic substitution of the nitro-group by the hydroxyl took place and the bicyclic-compound **20** was obtained as the final product.

2-[4-(1*H*-imidazol-1-yl)phenyl]-1-(3-nitro-1*H*-1,2,4-triazol-1-yl)propan-2-ol (**14**). Off-white powder (15%): mp 133–134 °C; 1H NMR [500 MHz, $(CD_3)_2CO$] δ 8.47 (s, 1H), 8.06 (s, 1H), 7.72 (d, $J = 8.5$ Hz, 2H), 7.60 (d, $J = 8.5$ Hz, 2H), 7.58 (s, 1H), 7.10 (s, 1H), 5.09 (s, 1H), 4.69 (d, $J = 4.5$ Hz, 2H), 1.68 (s, 3H). HRESIMS calcd for $C_{14}H_{15}N_6O_3$ m/z $[M + H]^+$ 315.1200, found 315.1207.

2-[4-(1*H*-imidazol-1-yl)phenyl]-1-(1*H*-1,2,4-triazol-1-yl)propan-2-ol (**15**). White powder (32%): mp 138–140 °C; 1H NMR [500 MHz, $(CD_3)_2CO$] δ 8.20 (s, 1H), 8.05 (s, 1H), 7.80 (s, 1H), 7.66 (d, $J = 8.5$ Hz, 2H), 7.56 (d, $J = 8.5$ Hz, 2H), 7.10 (s, 1H), 4.89 (s, 1H), 4.54 (d, $J = 4.0$ Hz, 2H), 1.57 (s, 3H). HRESIMS calcd for $C_{14}H_{16}N_5O$ m/z $[M + H]^+$ 270.1349, found 270.1363.

2-(4-Phenylphenyl)-1-(1*H*-1,2,4-triazol-1-yl)propan-2-ol (**16**). White powder (37%; based on recovered ketone the yield was 50%): mp 118–120 °C; 1H NMR [500 MHz, $(CD_3)_2CO$] δ 8.20 (s, 1H), 7.81 (s, 1H), 7.67–7.61 (m, 6H), 7.45 (t, $J = 7.5$ Hz, 2H), 7.35 (t, $J = 7.5$ Hz, 1H), 4.79 (s, 1H), 4.43 (s, 2H), 1.55 (s, 3H). HRESIMS calcd for $C_{17}H_{18}N_3O$ m/z $[M + H]^+$ 280.1444, found 280.1453.

1-(3-Nitro-1*H*-1,2,4-triazol-1-yl)-2-(4-phenylphenyl)propan-2-ol (**17**). White powder (19%): mp was not determined; 1H NMR (500 MHz, $CDCl_3$) δ 8.17 (s, 1H), 7.63–7.58 (m, 4H), 7.51–7.44 (m, 4H), 7.38 (t, $J = 7.0$ Hz, 1H), 4.52 (d, $J = 3.5$ Hz, 2H), 1.67 (s, 3H). HRESIMS calcd for $C_{17}H_{16}N_4NaO_3$ m/z $[M + Na]^+$ 347.1115, found 347.1124.

2-(2,4-Difluorophenyl)-1-(3-nitro-1*H*-1,2,4-triazol-1-yl)-3-(1*H*-1,2,4-triazol-1-yl)propan-2-ol (**18**). White powder (25%): mp 154–156 °C; 1H NMR (400 MHz, $CDCl_3$) δ 8.32 (s, 1H), 7.94 (s, 1H), 7.87 (s, 1H), 7.42 (ddd, $J = 8.8, 6.4, 2.4$ Hz, 1H), 6.88–6.79 (m, 2H), 5.66 (s, 1H), 4.99 (d, $J = 14.4$ Hz, 1H), 4.76 (d, $J = 14.4$ Hz, 1H), 4.64 (d, $J = 14.0$ Hz, 1H), 4.34 (d, $J = 14.0$ Hz, 1H). HRESIMS calcd for $C_{13}H_{19}F_2N_7O_3$ m/z $[M + H]^+$ 352.09697, found 352.0980.

1-(3-Nitro-1*H*-1,2,4-triazol-1-yl)-2-(4-phenylphenyl)-3-(1*H*-1,2,4-triazol-1-yl)propan-2-ol (**19**). White powder (33%): mp 90–93 °C (dec); 1H NMR [500 MHz, $(CD_3)_2CO$] δ 8.46 (s, 1H), 8.23 (s, 1H), 7.86 (s, 1H), 7.65–7.60 (m, 6H), 7.45 (t, $J = 8.0, 2$ Hz), 7.36 (t, $J = 7.5, 1$ Hz), 5.57 (s, 1H), 4.98 (d, $J = 14.0, 1$ Hz), 4.95 (d, $J = 14.0, 1$ Hz), 4.91 (d, $J = 14.0, 1$ Hz), 4.79 (d, $J = 14.0, 1$ Hz). HRESIMS calcd for $C_{19}H_{18}N_7O_3$ m/z $[M + H]^+$ 392.1466, found 392.1469.

1-[[2-(2,4-Difluorophenyl)-2*H*,3*H*-imidazo[2,1-*b*][1,3]oxazol-2-yl]methyl]-1*H*-1,2,4-triazole (**20**). White powder (29%): mp 134–137 °C (dec); 1H NMR [500 MHz, $(CD_3)_2CO$] δ 8.35 (s, 1H), 7.72 (s, 1H), 7.49 (ddd, $J = 17.5, 9.0, 6.5$ Hz, 1H), 7.21 (ddd, $J = 11.5, 9.0, 2.5$ Hz, 1H), 7.05 (dddd, $J = 11.5, 9.0, 3.0, 1.0$ Hz, 1H), 6.66 (d, $J = 1.5$ Hz, 1H), 6.51 (d, $J = 1.5$ Hz, 1H), 5.04 (d, $J = 15.0$ Hz, 1H), 4.95 (d, $J = 15.0$ Hz, 1H), 4.88 (dd, $J = 11.0, 2.0$ Hz, 1H), 4.46 (dd, $J = 11.0, 2.0$ Hz, 1H). HRESIMS calcd for $C_{14}H_{12}F_2N_5O$ and $C_{14}H_{11}F_2N_5NaO$ m/z $[M + H]^+$ and $[M + Na]^+$ 304.1004 and 326.0824, found 304.1006 and 326.0829.

4-Methyl-*N*-[1-(3-nitro-1*H*-1,2,4-triazol-1-yl)-3-phenylpropan-2-yl]benzene-1-sulfonamide (**21**). 3-Nitro-1,2,4-triazole (0.68 mmol) was dissolved in dry 1-propanol (5 mL), and then NaH (60%, 1.05 equiv) was added. Then the commercially available (Aldrich) *S*-(+)-2-benzyl-1-(*p*-tosylaziridine) (0.68 mmol) was added, and the reaction mixture was refluxed for 6 h. The reaction mixture was chromatographed on silica gel plates with ethyl acetate/petroleum ether (60:40) as eluent. White crystals (36%): mp 147–148 °C; 1H NMR (400 MHz, $CDCl_3$) δ 8.18 (s, 1H), 7.43 (d, $J = 8.0$ Hz, 2H), 7.26 (m, 3H),

7.18 (d, $J = 8.0$ Hz, 2H), 7.00 (m, 2H), 4.64 (d, $J = 7.2$ Hz, 1H), 4.54 (dd, $J = 14.0, 4.0$ Hz, 1H), 4.20 (dd, $J = 14.8, 6.8$ Hz, 1H), 3.83 (m, 1H), 2.96 (dd, $J = 14.8, 6.8$ Hz, 1H), 2.75 (dd, $J = 14.4, 7.2$ Hz, 1H), 2.42 (s, 3H). HRESIMS calcd for $C_{18}H_{20}N_5O_4S$ m/z $[M + H]^+$ 402.1231, found 402.1235.

1-(4-(2-Methyloxiran-2-yl)phenyl)-1H-imidazole (22). This compound was isolated during the synthesis of compound 14. White crystals (17%): mp 79–81 °C; 1H NMR [500 MHz, $(CD_3)_2CO$] δ 8.05 (s, 1H), 7.58 (d, $J = 8.5$ Hz, 2H), 7.56 (s, 1H), 7.53 (d, $J = 8.5$ Hz, 2H), 3.00 (d, $J = 5.5$ Hz, 1H), 2.77 (d, $J = 5.5$ Hz, 1H), 1.71 (s, 3H). HRESIMS calcd for $C_{12}H_{13}N_2O$ m/z $[M + H]^+$ 201.1022, found 201.1024.

Biological Evaluation. Animal studies were approved by the Institutional Animal Care and Use Committee of New York University School of Medicine (protocol #81213). This protocol adheres to the guidelines of the Association for Assessment and Accreditation of Laboratory Animal Care International (AAALAC).

In Vitro Screening. *In vitro* activity against *T. cruzi*, *T. b. rhodesiense*, and cytotoxicity assessment using L6 cells (rat skeletal myoblasts) was determined using a 96-well plate format as previously described.³² Data were analyzed with the graphic program Softmax Pro (Molecular Devices, Sunnyvale, CA, USA), which calculated IC_{50} values by linear regression from the sigmoidal dose inhibition curves.

Enzymatic Activity Studies with Type I NTR. Recombinant TbNTR was prepared and assayed as previously described.^{33,34} The activity of purified his-tagged TbNTR was assessed spectrophotometrically at 340 nm using various nitrotriazole substrates (100 μM) and NADH (100 μM) and expressed as nmol NADH oxidized $min^{-1} mg^{-1}$ of enzyme.

Testing *T. cruzi* CYP51 as a Potential Inhibition Target. Selected compounds (2, 18, and 19) were evaluated as CYP51 ligand/inhibitors using purified full-length *T. cruzi* CYP51 protein sample.²⁸ Binding affinities of the compounds were estimated using spectral titration. The experiments were performed on a dualbeam Shimadzu UV-240IPC spectrophotometer in the wavelength range 350–450 nm at 25 °C in 2 mL tandem cuvettes at 2 μM P450 and ligand concentrations ranging from 0.5 to 10 μM . The apparent dissociation constants were calculated by plotting the absorbance changes in the difference spectra ($\Delta A_{425-390}$) upon titration against free ligand concentration and fitting the data to a rectangular hyperbola in Sigma Plot Statistics. Inhibitory potencies of the compounds were compared in the reconstituted CYP51 reaction 5 min and 1 h, at 50/2/1 molar ratio substrate/inhibitor/enzyme. P450 concentration in the reaction mixture was 1 μM . The reaction products were analyzed on a reverse-phase HPLC system (Waters) equipped with a C18Nova Pak column and a β -RAM detector (INUS Systems, Inc.).⁹

In Vivo Antichagasic Activity Assessment of Selected Compounds. For *in vivo* studies, a Brazilian strain trypanomastigotes from transgenic *T. cruzi* parasites expressing firefly luciferase were used as described before.¹⁹ Briefly, parasites were injected in Balb/c mice (10^5 trypanomastigotes per mouse), and 3 days later mice were anesthetized by inhalation of isoflurane, followed by an injection with 150 mg/kg of D-luciferin potassium-salt in PBS. Mice were imaged 5 to 10 min after injection of luciferin with an IVIS 100 (Xenogen, Alameda, CA), and the data acquisition and analysis were performed with the software LivingImage (Xenogen) as described before.³⁵ Treatment with test compounds was started 4 days after infection at a specific concentration (usually 15 mg/kg/day \times 10 days) by i.p. injection. The vehicle control was 2% methylcellulose + 0.5% Tween 80 and groups of 5 mice/group were used. In the vehicle control group, 10 mice were used. Mice were imaged on days 5 and 10 as above. Parasite index was calculated as the ratio of parasite levels in treated mice compared to the control group and multiplied by 100. The ratio of parasite levels is calculated for each animal dividing the luciferase signal after treatment by the luciferase signal on the first imaging (before treatment). Mean values of all animals in each group \pm SD were then used to calculate the parasite index.³⁵

In Vitro ADME Studies. ADME *in vitro* studies were performed by APREDICA (Watertown, MA). Samples were analyzed by LC/MS/MS using an Agilent 6410 mass spectrometer coupled with an Agilent

1200 HPLC and a CTC PAL chilled autosampler, all controlled by MassHunter software (Agilent). After separation on a C18 reverse phase HPLC column (Agilent, Waters, or equivalent) using an acetonitrile–water gradient system, peaks were analyzed by mass spectrometry (MS) using ESI ionization in MRM mode.

Microsomal Stability Screen. Each test compound was dissolved in DMSO and incubated (37 °C) at 1 μM final concentration with 0.3 mg/mL of microsomal protein in 100 mM potassium phosphate, 3 mM $MgCl_2$, pH 7.4, in the presence or absence of 2 mM NADPH (to detect NADPH-free degradation) for up to 60 min as has been described before.¹⁹ Data were reported as % remaining parent compound.

Caco-2 Monolayer Permeability Studies. Caco-2 cells grown in tissue culture flasks were trypsinized and suspended in medium, and the suspensions were applied to wells of a collagen-coated BioCoat Cell Environment in 96-well format. The cells were allowed to grow and differentiate for 3 weeks, feeding at 2-day intervals. For Apical to Basolateral (A \rightarrow B) permeability, the test agent was added to the apical (A) side at 10 μM final concentration, and the amount of permeation was determined on the basolateral (B) side after 2 h assay time as described before.¹⁹ Data were expressed as permeability (P_{app}): $P_{app} = (dQ/dt)/C_0A$, where dQ/dt is the rate of permeation, C_0 is the initial concentration of test agent, and A is the area of the monolayer.³¹

■ ASSOCIATED CONTENT

Supporting Information

Synthesis, spectroscopic data, and references of precursor chloroacetamides 1a–g. This material is available free of charge via the Internet at <http://pubs.acs.org>.

■ AUTHOR INFORMATION

Corresponding Author

*Tel: (847)570-2262. Fax: (847)570-1878. E-mail: mpapadopoulou@northshore.org.

Notes

The authors declare no competing financial interest.

■ ACKNOWLEDGMENTS

The authors thank M. Cal, S. Keller, and M. Jud (Swiss TPH) for parasite assay results and Dr. Ana Rodriguez (New York University School of Medicine) for obtaining the *in vivo* data. This work was supported in part by internal funds of the Radiation Medicine Department at NorthShore University HealthSystem. Experiments on *T. cruzi* CYP51 were funded by NIH (GM067871, to G.I.L.). *In vitro* screenings against parasites were funded by DNDi. For that project, DNDi received funding from the following donors: Department for International Development (DFID), U.K.; Bill & Melinda Gates Foundation (BMGF), USA; Reconstruction Credit Institution-Federal Ministry of Education and Research (KfW-BMBF), Germany; and Directorate-General for International Cooperation (DGIS), The Netherlands. B.A.-V. acknowledges financial support by FONDECYT Postdoctorado 3130364. The donors had no role in study design, data collection and analysis, decision to publish, or preparation of the manuscript.

■ ABBREVIATIONS USED

NTD, Neglected tropical diseases; *T. cruzi*, *Trypanosoma cruzi*; *T. brucei*, *Trypanosoma brucei*; HAT, human African trypanosomiasis; Nfx, nifurtimox (4-(5-nitrofururylindenamino)-3-methylthio-morpholine-1,1-dioxide); Bnz, benzimidazole (*N*-benzyl-2-(2-nitro-1*H*-imidazol-1-yl)acetamide); NTR, type I nitroreductase; TcNTR, *T. cruzi* NTR; TbNTR, *T. brucei* NTR; CYP51, sterol 14 α -demethylase enzyme; TcCYP51, *T. cruzi*

CYP51; IC₅₀, concentration for 50% growth inhibition; SI, selectivity index; SARs, structure–activity relationships; TDR, Tropical Diseases Research (<http://www.who.int/tdr/en/>)

■ REFERENCES

(1) Molyneux, D. H.; Hotez, P. J.; Fenwick, A. Rapid-Impact Interventions: How a Policy of Integrated Control for Africa's Neglected Tropical Diseases Could Benefit the Poor. *PLoS Med.* **2005**, *2*, e336.

(2) Rassi, A., Jr; Rassi, A.; Marin-Neto, J. A. Chagas disease (review). *Lancet* **2010**, *375*, 1388–1402.

(3) Leslie, M. Infectious diseases. A tropical disease hits the road. *Science* **2011**, *333*, 934.

(4) Gautret, P.; Clerinx, J.; Caumes, E.; Simon, F.; Jensenius, M.; Loutan, L.; Schlagenhauf, P.; Castelli, F.; Freedman, D.; Miller, A.; Bronner, U.; Parola, P. *Euro Surveill.* **2009**, *14*, 19327.

(5) Bern, C. Antitrypanosomal therapy for chronic Chagas' disease. *N. Engl. J. Med.* **2011**, *364*, 2527–2534.

(6) Fabbro, D. L.; Streiger, M. L.; Arias, E. D.; Bizai, M. L.; del Barco, M.; Amicone, N. A. Trypanocidal treatment among adults with chronic Chagas disease living in Santa Fe city (Argentina), over a mean follow-up of 21 years: parasitological, serological and clinical evaluation. *Rev. Soc. Bras. Med. Trop.* **2007**, *40*, 1–10.

(7) Urbina, J. A. Ergosterol biosynthesis and drug development for Chagas disease. *Mem. Inst. Oswaldo Cruz* **2009**, *104* (Suppl1), 311–318.

(8) Keenan, M.; Abbott, M. J.; Alexander, P. W.; Armstrong, T.; Best, W. M.; Berven, B.; Botero, A.; Chaplin, J. H.; Charman, S. A.; Chatelain, E.; von Geldern, T. W.; Kerfoot, M.; Khong, A.; Nguyen, T.; McManus, J. D.; Morizzi, J.; Ryan, E.; Scandale, I.; Thompson, R. A.; Wang, S. Z.; White, K. L. Analogues of fenarimol are potent inhibitors of Trypanosoma cruzi and are efficacious in a murine model of Chagas disease. *J. Med. Chem.* **2012**, *55*, 4189–4204.

(9) Lepesheva, G. I.; Ott, R. D.; Hargrove, T. Y.; Kleshchenko, Y. Y.; Schuster, I.; Nes, W. D.; Hill, G. C.; Villalta, F.; Waterman, M. R. Sterol 14alpha-demethylase as a potential target for antitrypanosomal therapy: enzyme inhibition and parasite cell growth. *Chem. Biol.* **2007**, *14*, 1283–1293.

(10) Hargrove, T. Y.; Kim, K.; Soeiro, M. D. C.; da Silva, C. F.; Batista, D. D. J.; Batista, M. M.; Yazlovitskaya, E. M.; Waterman, M. R.; Sulikowski, G. A.; Lepesheva, G. I. Cyp51 structures and structure-based development of novel, pathogen-specific inhibitory scaffolds. *Int. J. Parasitol. Drugs Drug Resist.* **2012**, *2*, 178–186.

(11) Villalta, F.; Dobish, M. C.; Nde, P. N.; Kleshchenko, Y. Y.; Hargrove, T. Y.; Johnson, C. A.; Waterman, M. R.; Johnston, J. N.; Lepesheva, G. I. VNI Cures Acute and Chronic Experimental Chagas Disease. *J. Infect. Dis.* **2013**, *208*, 504–511.

(12) Andriani, G.; Amata, E.; Beatty, J.; Clements, Z.; Coffey, B. J.; Courtemanche, G.; Devine, W.; Erath, J.; Juda, C. E.; Wawrzak, Z.; Wood, J. T.; Lepesheva, G. I.; Rodriguez, A.; Pollastri, M. P. Antitrypanosomal lead discovery: Identification of a ligand-efficient inhibitor of Trypanosoma cruzi CYP51 and parasite growth. *J. Med. Chem.* **2013**, *56*, 2556–2567.

(13) Molina, I.; Prat, J. G.; Salvador, F.; Treviño, B.; Sulleiro, E.; Serre, N.; Pou, D.; Roue, S.; Cabezas, J.; Valerio, L.; Blanco-Grau, A.; Sánchez-Montalvá, A.; Vidal, X.; Pahissa, A. Randomized trial of posaconazole and benznidazole for chronic Chagas' disease. *N. Engl. J. Med.* **2014**, *370*, 1899–1907.

(14) Moraes, C. B.; Giardini, M. A.; Kim, H.; Franco, C. H.; Araujo-Junior, A. M.; Schenkman, S.; Chatelain, E.; Freitas-Junior, L. H. Nitroheterocyclic compounds are more efficacious than CYP51 inhibitors against Trypanosoma cruzi: implications for Chagas disease drug discovery and development. *Sci. Rep.* **2014**, *4*, 4703–4714.

(15) Diniz, L. d. F.; Urbina, J. A.; de Andrade, I. M.; Mazzeti, A. L.; Martins, T. A. F.; Caldas, I. S.; Talvani, A.; Ribeiro, I.; Bahia, M. T. Benznidazole and posaconazole in experimental Chagas disease: Positive interaction in concomitant and sequential treatments. *PLoS Negl. Trop. Dis.* **2013**, *7*, e2367.

(16) Papadopoulou, M. V.; Bourdin Trunz, B.; Bloomer, W. D.; McKenzie, C.; Wilkinson, S. R.; Prasittichai, C.; Brun, R.; Kaiser, M.; Torreale, E. Novel 3-nitro-1H-1,2,4-triazole-based aliphatic and aromatic amines as anti-Chagasic agents. *J. Med. Chem.* **2011**, *54*, 8214–8223.

(17) Papadopoulou, M. V.; Bloomer, W. D.; Rosenzweig, H. S.; Chatelain, E.; Kaiser, M.; Wilkinson, S. R.; McKenzie, C.; Ioset, J.-R. Novel 3-nitro-1H-1,2,4-triazole-based amides and sulfonamides as potential anti-trypanosomal agents. *J. Med. Chem.* **2012**, *55*, 5554–5565.

(18) Papadopoulou, M. V.; Bloomer, W. D.; Rosenzweig, H. S.; Kaiser, M.; Chatelain, E.; Ioset, J.-R. Novel 3-nitro-1H-1,2,4-triazole-bearing piperazines and 2-amino-benzothiazoles as anti-Chagasic agents. *Bioorg. Med. Chem.* **2013**, *21*, 6600–6607.

(19) Papadopoulou, M. V.; Bloomer, W. D.; Rosenzweig, H. S.; Ashworth, R.; Wilkinson, S. R.; Kaiser, M.; Andriani, G.; Rodriguez, A. Novel 3-nitro-1H-1,2,4-triazole-based compounds as potential anti-Chagasic drugs: *In vivo* studies. *Future Med. Chem.* **2013**, *5*, 1763–1776.

(20) Buchanan-Kilbey, G.; Djumpha, J.; Papadopoulou, M. V.; Bloomer, W. D.; Hu, L.; Wilkinson, S. R.; Ashworth, R. Evaluating the developmental toxicity of trypanocidal nitroaromatic compounds on zebrafish. *Acta Trop.* **2013**, *128*, 701–705.

(21) Wilkinson, S. R.; Taylor, M. C.; Horn, D.; Kelly, J. M.; Cheeseman, I. A mechanism for cross-resistance to nifurtimox and benznidazole in trypanosomes. *Proc. Natl. Acad. Sci. U.S.A.* **2008**, *105*, 5022–5027.

(22) Alsford, S.; Eckert, S.; Baker, N.; Glover, L.; Sanchez-Flores, A.; Leung, K. F.; Turner, D. J.; Field, M. C.; Berriman, M.; Horn, D. High-throughput decoding of antitrypanosomal drug efficacy and resistance. *Nature* **2010**, *482*, 232–236.

(23) Baker, N.; Alsford, S.; Horn, D. Genome-wide RNAi screens in African trypanosomes identify the nifurtimox activator NTR and the efloornithine transporter AAT6. *Mol. Biochem. Parasitol.* **2011**, *176*, 55–57.

(24) Wilkinson, S. R.; Bot, C.; Kelly, J. M.; Hall, B. S. Trypanocidal activity of nitroaromatic prodrugs: current treatments and future perspectives. *Curr. Top. Med. Chem.* **2011**, *11*, 2072–2084.

(25) Urbina, J. A. Specific treatment of Chagas disease: current status and new developments. *Curr. Opin. Infect. Dis.* **2001**, *6*, 733–741.

(26) Kim, Y. F.; Yoon, G. J.; Park, M. H. Preparation of fluconazole. *PCT Int. Appl.*, WO 9832744 A1 19980730, 1998.

(27) Nwaka, S.; Ramirez, B.; Brun, R.; Maes, L.; Douglas, F.; Ridley, R. Advancing drug innovation for neglected diseases—criteria for lead progression. *PLoS Negl. Trop. Dis.* **2009**, *3*, e440.

(28) Lepesheva, G. I.; Zaitseva, N. G.; Nes, W. D.; Zhou, W.; Arase, M.; Liu, J.; Hill, G. C.; Waterman, M. R. CYP51 from Trypanosoma cruzi: a phyla-specific residue in the B' helix defines substrate preferences of sterol 14alpha-demethylase. *J. Biol. Chem.* **2006**, *281*, 3577–8.

(29) Lepesheva, G. I.; Hargrove, T. Y.; Anderson, S.; Kleshchenko, Y.; Furtak, V.; Wawrzak, Z.; Villalta, F.; Waterman, M. R. Structural insights into inhibition of sterol 14alpha-demethylase in the human pathogen Trypanosoma cruzi. *J. Biol. Chem.* **2010**, *285*, 25582–25590.

(30) Lepesheva, G. I.; Hargrove, T. Y.; Kleshchenko, Y.; Nes, W. D.; Villalta, F.; Waterman, M. R. CYP51: A major drug target in cytochrome P450 superfamily. *Lipids* **2008**, *43*, 1117–1125.

(31) Stewart, B. H.; Chan, O. H.; Lu, R. H.; Reyner, E. L.; Schmid, H. L.; Hamilton, H. W.; Steinbaugh, B. A.; Taylor, M. D. Comparison of intestinal permeabilities determined in multiple *in vitro* and *in situ* models: Relationship to absorption in humans. *Pharm. Res.* **1995**, *12*, 693–699.

(32) Orhan, I.; Sener, B.; Kaiser, M.; Brun, R.; Tasdemir, D. Inhibitory activity of marine sponge-derived natural products against parasitic protozoa. *Mar. Drugs* **2010**, *8*, 47–58.

(33) Hall, B. S.; Wu, X.; Hu, L.; Wilkinson, S. R. Exploiting the drug-activating properties of a novel trypanosomal nitroreductase. *Antimicrob. Agents Chemother.* **2010**, *54*, 1193–1199.

(34) Hall, B. S.; Meredith, E. L.; Wilkinson, S. R. Targeting the substrate preference of a type I nitroreductase to develop anti-trypanosomal quinone-based prodrugs. *Antimicrob. Agents Chemother.* **2012**, *56*, 5821–5830.

(35) Andriani, G.; Chessler, A-D. C.; Courtemanche, G.; Burleigh, B. A.; Rodriguez, A. Activity *in vivo* of anti-trypanosoma *cruzi* compounds selected from a high throughput screening. *PLoS Negl. Trop. Dis.* **2011**, *5*, e1298.